ICIC Express Letters
Part B: Applications
Volume **15**, Number **2**, February **2024**

ICIC International ©2024 ISSN 2185-2766
pp. **147–154**

STEERING CONTROL FOCUSED ON SPEED CONTROL CONSIDERING DYNAMICS MODEL

Kaito Takayanagi[1], Kotaro Hashikura[2], Md Abdus Samad Kamal[2] and Kou Yamada[2]

[1]Graduate School of Science and Technology
[2]Division of Mechanical Science and Technology
Gunma University
1-5-1 Tenjincho, Kiryu 376-8515, Japan
{ t221b054; k-hashikura; maskamal; yamada }@gunma-u.ac.jp

Received May 2023; accepted July 2023

Abstract. *Vehicle operation can be divided into steering control and speed control. In a previous study, control performance was confirmed in a simulation in which steering control was applied to vehicle kinematics focusing on the linkage with speed control. In this study, the control performance of this steering control in the simulation including the dynamics model is confirmed. The actuator control layer is based on the motor dynamics of the Lego EV3 model described by Isobe et al. For the steering control, we compared the standard steering control and the steering control focusing on the cooperetion with the speed control, and confirmed the control performance in the simulation. When standard steering control was applied, a delay was observed. On the other hand, the steering control with the speed control did not cause any delay.*
Keywords: Steering control, Speed control, Path following method, Lego Mindstorm EV3, Motor dynamics, Automatic driving

1. **Introduction.** Japan is currently a hyper-aged society, and the proportion of the elderly in the population is expected to increase in the future. The number of traffic fatalities per 100,000 persons by age group in traffic accidents in 2020 increased as the age group increased from 60 years old, indicating that the proportion of accidents caused by the elderly tends to be higher than that of other age groups. Preventing traffic accidents caused by elderly drivers is a major issue for Japan in the future. Therefore, we consider the possibility of reducing the number of traffic accidents caused by the elderly through automated driving. In order for automatic driving to reduce accidents involving the elderly, it is necessary to prevent accidents by providing driving assistance and to create an environment in which the elderly can live without a car as a means of transportation after they have lost their driver's license. Studies on these issues include the functions of automatic driving required to prevent accidents [1] and whether or not the elderly can drive [2]. The causes of accidents involving elderly drivers include decreased attention span, decreased field of vision, delayed reactions, and erroneous operation. The first step in realizing these goals is to make automated vehicles available to those who cannot drive. In order to achieve these goals, it is first necessary to ensure that automated vehicles do not cause accidents. Automatic driving technology is attracting attention not only as a solution to the aging population problem, but also as a solution to environmental problems and driving safety issues. Automated driving has the effect of reducing the amount of unnecessary acceleration. When the driver is a human, the desire to get to the destination as quickly as possible during the commute to work causes the driver to accelerate more than necessary, which increases the amount of gas pedal operation, and the arrival time

DOI: 10.24507/icicelb.15.02.147

to the destination does not change significantly, but the amount of exhaust gas emissions increases. Therefore, automatic driving can suppress acceleration caused by unnecessary gas pedal operation. To improve safety in driving by automatic driving, the vehicle-maintaining autocruise as described in [3] can prevent rear-end collisions by maintaining a constant distance from the car in front, and can also prevent road rage, which is one of the dangerous driving problems that have recently become an issue.

Although we have just mentioned the advantages of automated driving, the opposite dangers include vulnerability to hacking, vulnerability to sensing in bad weather, and high impact due to communication failures. Research on automated driving has been conducted extensively, including the use of digital maps to estimate the vehicle's self-position [4, 5], planning to determine the trajectory to be traveled [6, 7, 8] and hazard prediction [9], and has been applied to vehicles already on the market, such as driver assistance assist, false start suppression, and vehicle lane keeping. Path following control is required for automatic vehicles to follow a generated trajectory in order to drive safely. The research on path following includes [10, 11, 12]. Preview control improves lane keeping performance when applied to driver assistance. Although [11] focused on preview control, there was a problem of deviation in the direction of the vehicle body. In previous study [13], the problem of [11] was solved by using H^2 control, which can be applied to preview control. However, when the control in previous study [13] was applied to a motor model, the control performance decreased. Therefore, the purpose of this study is to solve the control performance decrease when the motor dynamics are considered. In this study, the method of [14] is applied as motor control to solving the control performance decrease when motor dynamics are considered.

This paper is organized as follows. In Section 2, we derive two types of steering control for the vehicle applied in the simulation. Section 3 describes the vehicle motion control and shows the actuator control. Section 4 compares the results of the standard steering control [15] obtained by simulation with the steering control based on the method in [13]. Section 5 presents the conclusions.

2. **Steering Control.** In this section, the path following method is used to derive the error system for the reference state and the current state according to the path following method [16]. There is a mobile robot which is located on a 2-dimensional plane in which a global Cartesian coordinate system is defined. The vehicle possesses three degrees of freedom in its positioning which are represented as

$$p = \begin{bmatrix} x \\ y \\ \phi \end{bmatrix} \tag{1}$$

When there exist $\dot{x}(t)$, $\dot{y}(t)$ (time t derivatives of $x(t)$, $y(t)$), ϕ is represented by the following function.

$$\phi(t) = \arctan\left(\frac{\dot{y}(t)}{\dot{x}(t)}\right) \tag{2}$$

In this control system, two postures use the reference posture p_{ref}.

$$p_{ref} = \begin{bmatrix} x_{ref} \\ y_{ref} \\ \phi_{ref} \end{bmatrix} \tag{3}$$

A reference posture is a goal posture of the vehicle and a current posture is its "real" posture at this moment, respectively. Figure 1 represents the error between the reference vehicle and the actual vehicle on the reference track.

Figure 2 represents a two-wheeled vehicle model with vehicle speed $V(t)$, slip angle $\beta(t)$, and yaw rate $r(t)$.

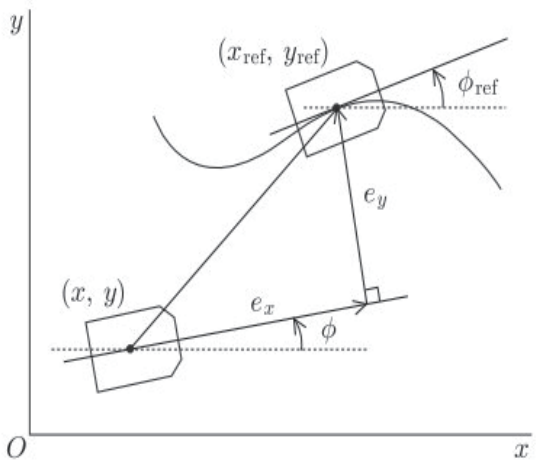

FIGURE 1. Relationship between actual and reference vehicles

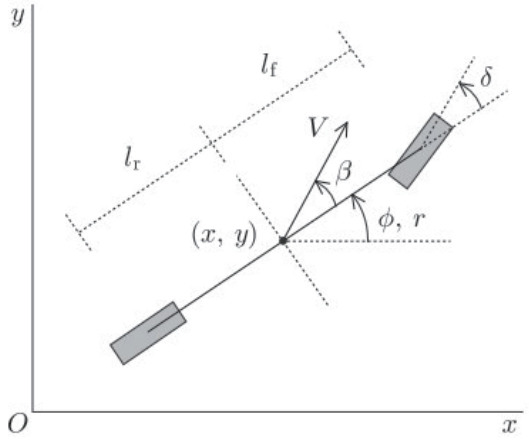

FIGURE 2. Two wheeled vehicle model

The current vehicle motion is expressed by the following differential equation.

$$\begin{bmatrix} \dot{x} \\ \dot{y} \\ \omega \end{bmatrix} = \dot{p}(t) = \begin{bmatrix} V(t)\cos(\phi(t)+\beta(t)) \\ V(t)\sin(\phi(t)+\beta(t)) \\ r(t) \end{bmatrix} \tag{4}$$

The reference vehicle is likewise a differential equation as follows:

$$\begin{bmatrix} \dot{x}_{ref}(t) \\ \dot{y}_{ref}(t) \\ \omega_{ref}(t) \end{bmatrix} = \dot{p}_{ref}(t) = \begin{bmatrix} V_{ref}(t)\cos\phi_{ref}(t) \\ V_{ref}(t)\sin\phi_{ref}(t) \\ \omega_{ref}(t) \end{bmatrix} \tag{5}$$

The cross track error between vehicles is obtained by the equation.

$$p_e = \begin{bmatrix} x_e \\ y_e \\ \phi_e \end{bmatrix} = \begin{bmatrix} R^T(\phi(t)) & 0 \\ 0 & 1 \end{bmatrix} \begin{bmatrix} x_{ref}(t)-x(t) \\ y_{ref}(t)-y(t) \\ \phi_{ref}(t)-\phi(t) \end{bmatrix} \begin{bmatrix} \cos\phi(t) & \sin\phi(t) & 0 \\ -\sin\phi(t) & \cos\phi(t) & 0 \\ 0 & 0 & 1 \end{bmatrix} \tag{6}$$

From the cross track error, the error system is derived as the following equation.

$$\dot{p_e} = \begin{bmatrix} \dot{x_e} \\ \dot{y_e} \\ \omega_e \end{bmatrix} \begin{bmatrix} r(t)y_e(t) + V_{ref}(t)\cos\phi_e(t) - V(t)\cos\beta(t) \\ -r(t)x_e(t) + V_{ref}(t)\sin\phi_e(t) - V(t)\sin\beta(t) \\ r_{ref}(t) - r(t) \end{bmatrix} \tag{7}$$

2.1. **Speed and steering control.** Next, explain steering control method from cross track error (7). In this chapter, we design the steering system of the vehicle from the error system derived earlier. In the tracking control, the steering control system of the vehicle takes as input the position $x_{ref}(t)$, $y_{ref}(t)$ and $\phi_{ref}(t)$ of the reference vehicle and the position of the current vehicle $x(t)$, $y(t)$ and $\phi(t)$ that are output from the vehicle kinematics. Then, $V_{cmd}(t)$ and $\omega_{cmd}(t)$ are output to the actuator control. When controlling an automobile, speed control and steering control are often performed separately, but this control system focuses on the cooperetion of the two. The error system between the reference vehicle and the actual vehicle is expressed by the equation where assuming $x_e = 0$, the actual vehicle speed V is expressed as follows:

$$V = \frac{1}{\cos\beta}\left(\omega y_e + V_{ref}\cos\phi_e\right) \tag{8}$$

If $\dot{x_e}(t) = 0$, $x_e(0) = 0$ is satisfied, then

$$x_e = 0 \tag{9}$$

at all time t, and the deviation in the direction of the car body can be suppressed. Furthermore, if $\beta = 0$, ϕ_e is small, the error system can be treated as the following equation.

$$V = \omega y_e + V_{ref}\cos\phi \tag{10}$$

$$\begin{bmatrix}\dot{y_e}\\ \dot{\phi_e}\end{bmatrix} = \begin{bmatrix}0 & V_{ref}\\ 0 & 0\end{bmatrix}\begin{bmatrix}y_e\\ \phi_e\end{bmatrix} + \begin{bmatrix}0\\ 1\end{bmatrix}\omega_{ref} + \begin{bmatrix}0\\ -1\end{bmatrix}\omega \tag{11}$$

2.2. **Standard steering control.** In standard steering control, the following control law is used to determine the vehicle velocity $V(t)$ and angular velocity $\omega(t)$.

$$V = \frac{V_R + V_L}{2} \tag{12}$$

$$\omega = \frac{V_R - V_L}{2d} \tag{13}$$

Here, V_R and V_L are obtained as follows:

$$V = \rho\omega \tag{14}$$

$$V_R = (\rho + d)\dot{\phi} \tag{15}$$

$$V_L = (\rho - d)\dot{\phi} \tag{16}$$

Let ρ be the inclination of the car body ρ, and d the center of the car body from the wheels.

3. Application to Vehicle Control.

3.1. **Hierachical structure of robot.** Although the steering control was designed, the motion control of a two-wheeled vehicle is divided into a steering control layer and an actuator control layer as shown in Figure 3 [17]. The steering control layer calculates the error between the reference vehicle running on the generated path and the actual vehicle, and outputs control quantities, in this case velocity and angular velocity. In the actuator control layer, the speed and angular velocity inputs from the steering control layer are converted to voltage and output to the motors. The vehicle model uses two wheels, each with a DC motor with a rotary encoder. It is assumed that the angle of rotation can be obtained from them. The approximate derivative of this rotation angle is the angular velocity of the vehicle and is input to the steering control layer.

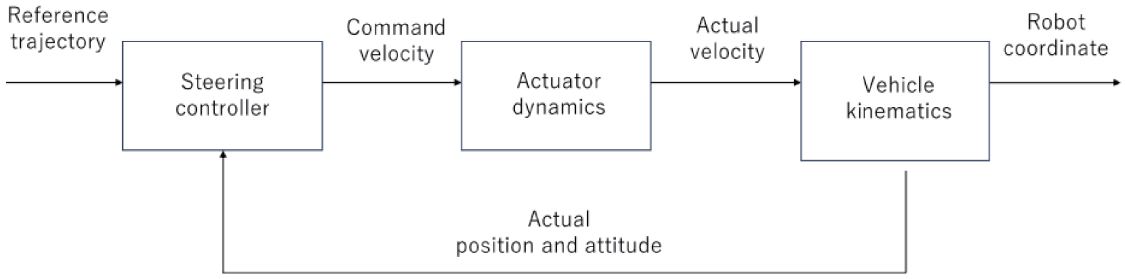

FIGURE 3. Hierachical structure of robot

3.2. **Motor control.** In this section, we explain the motor dynamics model applied to a vehicle model. When conducting vehicle experiments, it is first necessary to verify the performance of the control by using an easy-to-handle vehicle model, rather than applying it to a car. In this study, the Lego EV3 dynamics model is used as the vehicle model. The motor control is treated as the motor control with servo compensation as described in [14]. The equations of motion are as follows:

$$\begin{aligned}
&\begin{bmatrix} \frac{Mr^2}{4}+\frac{Ir^2}{L^2}+J & \frac{Mr^2}{4}-\frac{Ir^2}{L^2} \\ \frac{Mr^2}{4}-\frac{Ir^2}{L^2} & \frac{Mr^2}{4}+\frac{Mr^2}{4}+\frac{Ir^2}{L^2}+J \end{bmatrix} \begin{bmatrix} \ddot{\theta}_1(t) \\ \ddot{\theta}_2(t) \end{bmatrix} \\
&= \begin{pmatrix} \frac{-n^2K_bK_t}{R_m} & 0 \\ 0 & \frac{-n^2K_bK_t}{R_m} \end{pmatrix} \begin{pmatrix} \dot{\theta}_1(t) \\ \dot{\theta}_2(t) \end{pmatrix} + \begin{pmatrix} \frac{nK_t}{R_m} & 0 \\ 0 & \frac{nK_t}{R_m} \end{pmatrix} \begin{pmatrix} u_1(t) \\ u_2(t) \end{pmatrix}
\end{aligned} \tag{17}$$

Let V and ω be the outputs of the system, expressed as

$$\begin{aligned}
&\begin{pmatrix} \ddot{\theta}_1(t) \\ \ddot{\theta}_2(t) \end{pmatrix} = A \begin{pmatrix} \dot{\theta}_1(t) \\ \dot{\theta}_2(t) \end{pmatrix} + B \begin{pmatrix} u_1(t) \\ u_2(t) \end{pmatrix} \\
&\begin{pmatrix} V \\ \omega \end{pmatrix} = C \begin{pmatrix} \dot{\theta}_1(t) \\ \dot{\theta}_2(t) \end{pmatrix} \\
&A = \begin{pmatrix} \frac{Mr^2}{4}+\frac{Ir^2}{L^2}+J & \frac{Mr^2}{4}-\frac{Ir^2}{L^2} \\ \frac{Mr^2}{4}-\frac{Ir^2}{L^2} & \frac{Mr^2}{4}+\frac{Ir^2}{L^2}+J \end{pmatrix}^{-1} \begin{pmatrix} \frac{n^2K_bK_t}{R_m} & 0 \\ 0 & \frac{-n^2K_bK_t}{R_m} \end{pmatrix} \\
&B = \begin{pmatrix} \frac{Mr^2}{4}+\frac{Ir^2}{L^2}+J & \frac{Mr^2}{4}-\frac{Ir^2}{L^2} \\ \frac{Mr^2}{4}-\frac{Ir^2}{L^2} & \frac{Mr^2}{4}+\frac{Ir^2}{L^2}+J \end{pmatrix}^{-1} \begin{pmatrix} \frac{nK_t}{R_m} & 0 \\ 0 & \frac{nK_t}{R_m} \end{pmatrix} \\
&C = \begin{pmatrix} \frac{r}{2} & \frac{r}{2} \\ \frac{r}{L} & -\frac{r}{L} \end{pmatrix}
\end{aligned} \tag{18}$$

The parameters of this motor are represented in Table 1.

TABLE 1. Parameters of vehicle model

$\frac{K_t}{R_m}$	Torque constant/Electric constant	0.2176 [N·m/AΩ]
K_b	EMF constant of motor	0.4283 [V·s/rad]
J_m	Motor moment of interia	5.912e^{-3} [kg·m^2]
M	Mass	0.675 [kg]
r	Wheel radius	0.0335 [m]
n	Geer ratio	1

4. Simulation.

4.1. **Condition of simulation.** The simulations performed in this study compare the results of the standard steering control method [15] and the control method [13] derived in Chapter 3.

(a)
$$V_{ref} = 0.05 \text{ [m/s]}$$

(b)
$$V_{ref} = 0.15 \text{ [m/s]}$$

4.2. **Simulation result.** In this study, vehicle steering control, vehicle dynamics, and motor dynamics were designed as shown in Figure 3. Therefore, to compare the steering control, we performed simulations with the steering control derived in [15] and Chapter 3. The dotted line in the graph represents the reference vehicle path. On the other hand, the solid line represents the actual vehicle model. Figure 6 shows that in the standard steering control, the virtual vehicle lags behind the dotted line representing the trajectory of the reference vehicle by about 0.5 [m] around 2.5 [m] on the x-axis. On the other hand, Figure 7 shows that the new steering control catches up with the reference vehicle at about 1.5 [m] on the x-axis, and is able to follow it without delay. Figure 4 and Figure 5 show the results of the simulation at a velocity of 0.05 [m/s]. The vehicle taraveled from upper left to lower right. Comparing the final point at the bottom right, Figure 4 shows a deviation of 0.5 [m]. On the other hand, in Figure 5 the solid line overlaps the dotted line and the deviation suppressed.

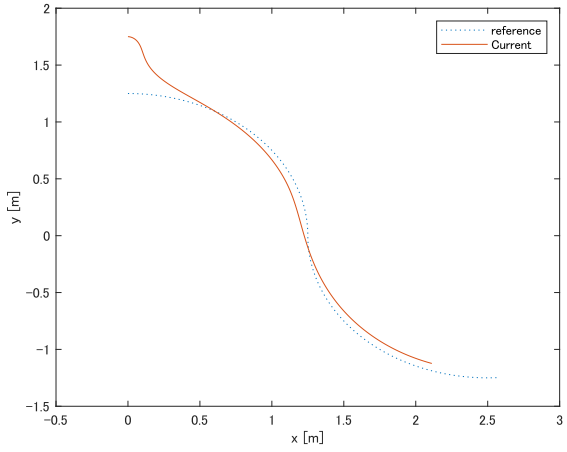

FIGURE 4. Standard steering control method (0.05 [m/s])

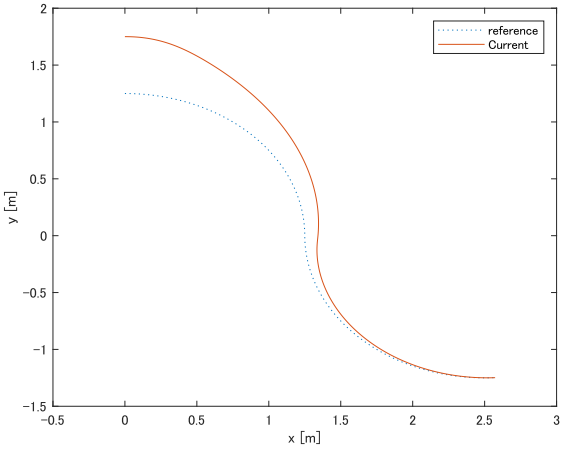

FIGURE 5. Proposed method (0.05 [m/s])

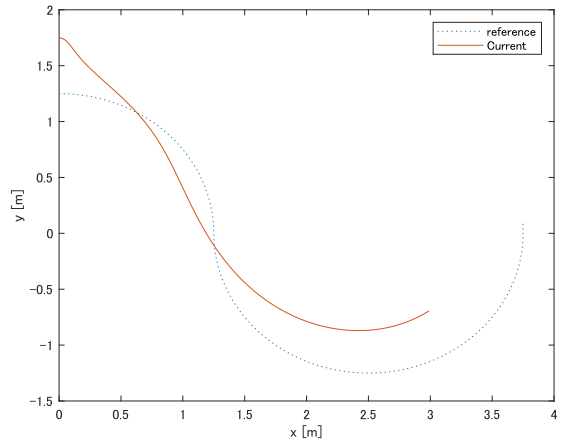

FIGURE 6. Standard steering control (0.15 [m/s])

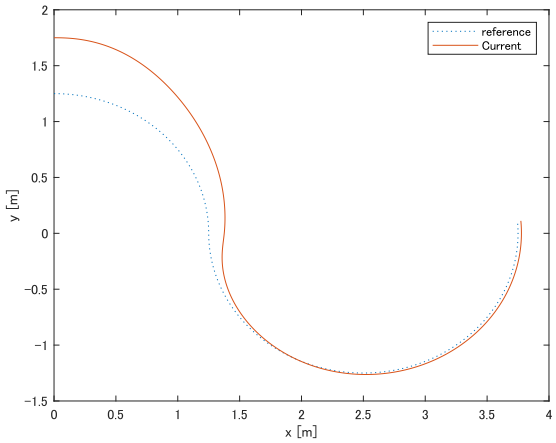

FIGURE 7. Proposed method (0.15 [m/s])

5. **Conclusions.** This study was conducted to solve the problem of control performance decrease when considering motor dynamics in steering control in a previous study [13].

Chapter 2 deals with the following control problem according to [16] and derives the control law of the vehicle [13] from the cross track error system. In Chapter 3, the equations of motion for the vehicle model considering the motor dynamics of [14] are presented. In the simulations, the standard steering control method [15] and the steering control method [13], which focuses on the cooperetion with the speed control, are compared. In the former case, the current vehicle lags behind the reference vehicle. On the other hand, when steering control method [13] was applied, it was confirmed that the current vehicle followed the reference vehicle without lagging behind. The simulation results show that the problem of control performance decrease when motor dynamics are considered in the control of the previous study [13] is solved. The future prospect is to confirm the control performance in actual vehicle experiments.

REFERENCES

[1] R. Shiokawa and M. Endou, Consideration about stopping traffic accident occurred by elderly people with automatic driving system, *JPAIS*, pp.178-181, 2018.

[2] E. Horikawa, Driving behavior and fitness to drive of older people, *The Japanese Journal of Rehabilitation Medicine*, vol.57, no.2, 2020.

[3] S. Takano and T. Kobayashi, Dvelopment of adaptive cruise control with brake control using network and fuzzy logic, *The Japan Society of Mechanical Engineers*, vols.4-7, 2004 (in Japanese).

[4] N. Suganuma and K. Yoneda, Utilization of digital map for autonomous vehicle, *RSJ*, vol.33, no.10, pp.760-765, 2015.

[5] S. Fujioka, T. Kashu, S. Yokokawa and T. Ozeki, Driving trajectory of autonomous driving based on HD map, *JSAE*, vol.53, no.5, 2022.

[6] Y. Makino, H. Yamaguchi and N. Yonezawa, Control of a 4-fork moving mechanism in an unknown environment without map information, *JSPE*, pp.513-514, 2022.

[7] S. Kishino, F. Sugasawa, T. Imaseki and H. Mouri, Research on path for autonomous vehicles based on acceleraration for collision avoidance, *JSAE*, vol.52, no.6, 2021.

[8] R. Cong, A. Fujiyama and T. Matsumoto, AI techniques aid for optimizing the collection system of industrial plastic waste, *SES*, vol.35, no.5, pp.248-257, 2022.

[9] K. Hashimoto, Y. Ishida, R. Ichise, H. Wagatsuma and H. Tamukoh, On-vehicle danger forecast system based on knowledge-based artificial inteligence, *ISCIE*, vol.31, no.5, 2018.

[10] R. Nakata, M. Tanemura and Y. Chida, Conditions for undershoot responses in circular path-following vehicle control with the rotational and expansionary coordinate transformation, *The Japan Society of Mechanical Engineers*, vol.88, no.913, 2022 (in Japanese).

[11] T. Yamamoto, K. Hashikura, M. A. S. Kamal and K. Yamada, Path following control of driver-vehicle system based on H^2 preview output feed back controller, *SICE Annual Conference*, pp.227-230, 2020.

[12] J. Wu, Q. Fu, Y. Liu and B. Sun, Trajectory following control for autonomous vehicles using the feedforward controller and the improved trajectory following model, *International Journal of Innovative Computing, Information and Control*, vol.17, no.6, pp.2019-2032, 2021.

[13] O. Bayarsaikhan, K. Takayanagi, K. Hashikura, M. A. S. Kamal and K. Kamada, Design of H^2 steering controller in corporation with speed control, *ICIC Express Letters*, vol.17, no.6, pp.667-674, 2023.

[14] M. Isobe, K. Hashikura, A. Kojima, M. A. S. Kamal and K. Yamada, Two-degree-of-freedom H_2 output regulation with application to trajectory tracking control, *IEEE Vehicle Power and Propulsion Conference (VPPC)*, pp.1-6, 2019.

[15] C. Gerald and F. Zhang, *Mobile Robots: Navigation, Control and Sensing, Surface Robots and AUVs*, Wiley-IEEE Press, 2020.

[16] Y. Kanayama, Y. Kimura, F. Miyazaki and T. Noguchi, A stable tracking control method for an autonomous mobile robot, *IEEE International Conference on Robotics and Automation*, pp.1236-1241, 1990.

[17] E. Nakano, K. Komoriya, K. Yoneda and T. Takahashi, *Highly Intelligent Mobile Robotics*, Koudansha, 2004 (in Japanese).